Short-range order and atomic diffusion in liquid Ge and $Si_{20}Ge_{80}$ investigated by neutron scattering and x-ray diffraction

H. Weis,[1,*] D. Holland-Moritz,[1,†] F. Kargl,[1] F. Yang,[1] T. Unruh,[2,‡] T. C. Hansen,[3] J. Bednarčik,[4,§] and A. Meyer[1]

[1]*Institut für Materialphysik im Weltraum, Deutsches Zentrum für Luft- und Raumfahrt (DLR), 51170 Köln, Germany*

[2]*Forschungsneutronenquelle Heinz Maier-Leibnitz (FRM II), Technische Universität München, 85747 Garching, Germany*

[3]*Institut Laue-Langevin, BP 156, 38042 Grenoble Cedex, France*

[4]*Deutsches Elektronen Synchrotron (DESY), Photon Science, Notkestr. 85, 22607 Hamburg, Germany*

(Received 10 September 2021; accepted 8 October 2021; published 25 October 2021)

We studied structure and dynamics in liquid Ge and $Si_{20}Ge_{80}$. Quasielastic neutron scattering (QNS) was employed to accurately determine the Ge self-diffusion coefficient. Static structure factors were measured using neutron and x-ray diffraction. Containerless processing via electromagnetic levitation (EML) enabled to obtain structure factors over a broad temperature range from the metastable regime of the undercooled melt to several hundred Kelvin above the melting point. Moreover, isotopic substitution and combination with x-ray diffraction allowed to determine the partial structure factors $S_{NN}(q)$, $S_{NC}(q)$, $S_{GeGe}(q)$, and $S_{GeSi}(q)$ for liquid $Si_{20}Ge_{80}$. The topological structures of liquid Ge and $Si_{20}Ge_{80}$ are very similar. In addition, the Ge self-diffusion coefficients in liquid Ge and $Si_{20}Ge_{80}$ are equal within error limits.

DOI: 10.1103/PhysRevB.104.134108

I. INTRODUCTION

Studies of the structure-dynamics relationship in metallic melts are essential to understand how the dynamical behavior of the constituents is controlled by structural differences on the atomic scale [1–5].

If the full set of partial structure factors is available for an alloy melt, the mode coupling theory (MCT) [6] of the glass transition is able to establish a firm relationship between the atomic structure and the atomic dynamics in the melt. While there are usually some deviations of the absolute values of the self-diffusion coefficients predicted by MCT, MCT has proven to be successful in describing relative changes of the dynamic properties. For instance, for Zr-Ni [5,7] and Hf-Ni [5,8] melts, the coupling/decoupling behavior of the self-diffusion coefficients of the different atomic species as well as the temperature dependence of the self-diffusion coefficients is well described by MCT taking the experimentally determined partial structure factors as an input.

So far, the relationship between the short-range structure and the atomic dynamics in liquid alloys has mainly been studied for systems consisting of metal atoms as the main component like Zr-Ni [5,7,9], Zr-Cu [10,11], Hf-Ni [5,8], Al-Ni [12], Ni-B [13], or Fe-C [14]. These are all densely packed melts characterized by predominantly metallic bonding.

In this work, we address melts of pure germanium (Ge) and of silicon-germanium (Si-Ge) alloys that are semiconducting in the solid state, showing a diamond-like structure where atoms are covalently bound with a coordination number of four. Upon melting Ge and Si-Ge undergo a semiconductor to metal transition. In the liquid state, the electrical conductivities are comparable to many liquid metals [15,16]. However, static structure factors reported for liquid Ge [17,18] exhibit a shoulder on the first diffraction maximum, a feature not visible in static structure factors of typical metallic liquids [19]. The coordination number of 5.6 derived from static structure factors in Ref. [18] lies significantly below coordination numbers in densely packed metallic liquids, with typical coordination numbers of about 12 or higher [5,19]. Moreover, the total static structure factors for Si-Ge alloys reported based on x-ray diffraction [20] and neutron diffraction [21] confirm the existence of a shoulder over the entire concentration range. Hence, the atomic arrangement in liquid Ge and Si-Ge is expected to be very different from that in densely packed metallic liquids.

Along with these differences in static structure, the atomic dynamics in liquid Ge and Si-Ge alloys are also expected to differ from those in densely packed metals. Ge self-diffusion coefficients in pure liquid Ge [22,23] and Ni self-diffusion in Si based Si-Ni alloys [24] as well as in $Ge_{66.7}Ni_{33.3}$ alloys [13] determined by quasielastic neutron scattering (QNS) are significantly higher at same temperature than diffusion coefficients in pure liquid metals (see Refs. [14,25,26] for liquid Cu, Ni and Fe) or densely packed metallic alloys like Zr-Ni(-Al) [5,9,27], Zr-Cu [10,11], Hf-Ni [5,8], Al-Ni [12], Ni-B [13], Fe-C [14], $Pd_{43}Ni_{10}Cu_{27}P_{20}$ [28], or Zr-Ti-Cu-Ni-Be [29].

*Present address: Department of Nuclear Medicine, Faculty of Medicine and University Hospital Cologne, University of Cologne, Cologne, Germany.

†dirk.Holland-Moritz@dlr.de

‡Present address: Lehrstuhl für Kristallographie und Strukturphysik, Friedrich-Alexander-Universität Erlangen-Nürnberg, Staudtstr. 3, 91058 Erlangen, Germany.

§Present address: Institute of Physics, Faculty of Science, P. J. Šafárik University in Košice, Park Angelinum 9, 04154 Košice, Slovakia.

 ©2021 American Physical Society

Numerous models were proposed to explain the relation of structure and dynamics in liquid Ge and Si-Ge. In Ref. [30], the static structure factor of liquid Ge is explained by a cluster-based approach in which tetrahedral clusters are assumed to prevail in the liquid. While the first principle peak in the structure factor is governed by the intercluster distances, the high-q part of the structure factor including the shoulder is dominated by the intracluster correlations. Hosokawa *et al.* [31] reported that the half width of the central lines of the dynamic structure factor shows significant narrowing at the position of the first maximum, supposedly representing slowly moving clusters, while there is considerably broadening near the shoulder, supposedly representing fast moving individual atoms. A deviation from an Arrhenius-like temperature dependence of the Ge self-diffusion coefficients in pure Ge reported in Ref. [32] is suggested to arise from the transition of a liquid containing tetrahedral clusters at lower temperatures to a more densely packed liquid at higher temperatures. Ab intio molecular dynamics (MD) simulations [33], on the other hand, revealed a broad distribution of coordination numbers between 3 and 8 close to the melting point, accompanied by a flat bond angle distribution with only a very flat maximum close to the tetrahedral bond angle. A similar bond angle distribution was reported in Ref. [34] at $T = 1250$ K. However at $T = 2000$ K, the bond angle distribution changed to one representing a more closely packed liquid, with no shoulder on the first diffraction peak of the static structure factor.

In the following, we address the structure dynamics relation in liquid Ge and $Si_{20}Ge_{80}$ based on results from neutron scattering and x-ray diffraction. Diffusion coefficients and static structure factors covering a broad temperature range above and below the melting point will be discussed. From an experimental point view, diffusion coefficients in liquid metals and semiconductors are commonly measured using the long capillary technique or its variants [35,36]. Here, a capillary with a typical diameter in the mm range is filled with a solid diffusion couple. Heated to the target temperature the liquid sample is annealed followed by cooling accompanied by solidification. Subsequently the resulting concentration profile is analyzed. However, buoyancy driven convective flow is expected to severely contribute to the mass transport in liquids. Errors in diffusion coefficients in the 100% range may be caused [37]. Additional systematic errors in capillary experiments result from segregation during melting, Marangoni convection caused by free surfaces and microstructure evolution during solidification [38].

Quasielastic neutron scattering (QNS) emerged as a complementary method to measure self-diffusion coefficients. Liquid dynamics is probed on a picosecond time - and on atomic length scale, thus leaving results unaffected by convection. Self-diffusion coefficients with errors below 10% are reported (see Refs. [26,26,39] for liquid Al, Cu, and Ni). In the following we will present measurements of Ge self-diffusion coefficients in liquid $Si_{20}Ge_{80}$ using QNS. We show that the Ge self-diffusion coefficients in liquid Ge and $Si_{20}Ge_{80}$ are equal within error limits.

Static structure factors in liquid metals have frequently been measured using both neutron and x-ray scattering [40]. In isotropic, monoatomic liquids one single structure factor completely describes the static structure. However, in binary liquids three partial structure factors are needed to fully describe the static structure. Combining neutron diffraction with isotopic substitution and x-ray diffraction we were able to determine good approximations of some of these partial structure factors for liquid $Si_{20}Ge_{80}$, the Bathia-Thornton partial structure factors $S_{NN}(q)$ and $S_{NC}(q)$ as well as the Faber-Ziman partial structure factors $S_{GeGe}(q)$ and $S_{GeSi}(q)$. Moreover, containerless processing via electromagnetic levitation (EML) enabled to measure structure factors for liquid Ge over a broad temperature range even in the metastable regime of the undercooled melt. Our results show that the topological structure in liquid Ge and $Si_{20}Ge_{80}$ is very similar.

II. EXPERIMENTAL DETAILS

The samples used for the neutron scattering and x-ray diffraction studies were prepared from high purity ^{nat}Ge purchased from PPM Pure Metals GmbH, ^{nat}Si (99.999%) purchased from Alfa Aesar, and ^{73}Ge Ge-isotope with a 99.40% isotope enrichment and metal impurities in the ppm range, purchased from STB Isotope Germany GmbH.

Samples with a mass of approximately 0.8 g were prepared for the experiments. Ge samples were cut from the Ge ingot. $Si_{20}Ge_{80}$ samples were alloyed by arc melting of the respective constituents under a high-purity argon atmosphere. With the exception of the QNS studies, all experiments were performed using electromagnetic levitation (EML) [41] under a high-purity atmosphere consisting of a mixture of helium and argon gas of 99.9999% purity.

Ge and $Si_{20}Ge_{80}$ are semiconductors in the solid state. At room temperature, the electrical conductivity is insufficient for the samples to couple to the electromagnetic field. Therefore a preheater was used to increase the electrical conductivity sufficiently for the samples to levitate, as described in Ref. [42]. Containerless processing under high-purity conditions enables to investigate the liquids over a broad temperature range even in the metastable regime of the undercooled melt by avoiding heterogeneous nucleation at container walls or impurity sites.

III. QUASIELASTIC NEUTRON SCATTERING STUDIES ON LIQUID $Si_{20}Ge_{80}$

The atomic dynamics in liquid $Si_{20}Ge_{80}$ were measured on the neutron time of flight spectrometer ToFToF at the FRM II in Garching, Germany. $Si_{20}Ge_{80}$ samples containing either ^{nat}Ge or a 1:1 mixture of ^{nat}Ge and ^{73}Ge were used. The ratio of incoherent to coherent scattering cross section is one order of magnitude higher for the isotope mixture with 0.22 than for ^{nat}Ge with 0.02. The measurements were performed in thin-walled Al_2O_3 containers inside the standard niobium resistance furnace of the FRM II in a temperature range of 1430 to 1693 K. An incoming neutron wavelength of 7 Å was chosen providing an accessible wavenumber range of 0.3 to 2.0 $Å^{-1}$ with an energy resolution of approximately 50 μeV full width at half maximum.

Ge self-diffusion coefficients in liquid $Si_{20}Ge_{80}$ were measured using QNS in a temperature range of approximately 30 to 300 K above the liquidus temperature. The measured time of flight spectra were normalized to a vanadium standard,

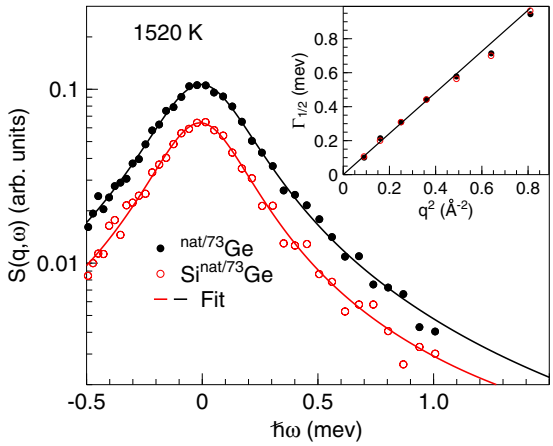

FIG. 1. Dynamic structure factor $S(q, \omega)$ of liquid Ge [22,23] and $Si_{20}Ge_{80}$ at a wave number of 0.4 Å^{-1}. The lines are fits with a Lorentzian function (1) convolved with the energy resolution function. The inset shows the q-dependent half width $\Gamma_{1/2}$ obtained from the fits to $S(q, \omega)$ as a function of q^2. The slope is proportional to the Ge-self diffusion coefficient.

corrected for self-absorption and empty container scattering, and interpolated to constant wave numbers q to obtain the dynamic structure factor $S(q, \omega)$.

In Fig. 1, the measured $S(q, \omega)$ is depicted at a wave number of 0.4 Å^{-1}. For comparison $S(q, \omega)$ obtained for liquid Ge is also shown, taken from Refs. [22,23]. All spectra can be well described by Lorentzian functions:

$$S(q,\omega) = \frac{A}{\pi}\frac{\Gamma(q)q^2}{(2\hbar\omega^2) + (\Gamma(q))^2} \otimes R(q,\omega) + b(q), \qquad (1)$$

convolved with the energy resolution function $R(q, \omega)$. Here, $b(q)$ denotes an energy independent background and $\Gamma(q)$ the half width at half maximum of the Lorentzian curve. The shapes of the QNS spectra of liquid Ge and $Si_{20}Ge_{80}$ are very similar.

Generally, in neutron scattering the scattering signal is proportional to the sum of the coherent and the incoherent part of the dynamic structure factor $S(q, \omega)$. For small q and within the observed energy range, the QNS spectra are dominated by the incoherent part of the scattering signal (see Refs. [23,25] for details). ^{nat}Ge exhibits an incoherent neutron scattering cross section σ_{inc} of 0.18 barn, the $^{73/nat}$Ge mixture $\sigma_{inc} = 1.2$ barn, and Si $\sigma_{inc} = 0.004$ barn. For additive incoherent scattering contributions, our spectra are dominated by Ge correlations and the Ge self-diffusion coefficients can be derived via [43]

$$D_s = \frac{\Gamma(q)}{2\hbar q^2}. \qquad (2)$$

In Fig. 2, Ge self-diffusion coefficients in liquid $Ge_{80}Si_{20}$ are depicted as obtained for samples containing ^{nat}Ge and the $^{nat/73}$Ge isotope mixture. Within the error limits the diffusion coefficients are similar, indicating that Ge self-correlations indeed dominate our spectra in case Ge and Si exhibit different mobilities. The Ge self-diffusion coefficients for pure liquid Ge [22,23] are also depicted. In Table I the measured diffusion coefficients are listed. As can be seen, the Ge self-

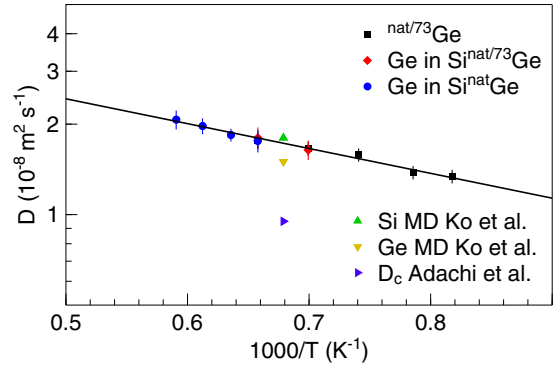

FIG. 2. Ge self-diffusion coefficient in liquid $Si_{20}Ge_{80}$ and liquid Ge [22,23] as a function of the inverse temperature, measured using QNS on Si_{20} $^{nat}Ge_{80}$ and Si_{20} $^{nat/73}Ge_{80}$ samples. ^{nat}Ge exhibits an incoherent neutron scattering cross section σ_{inc} of 0.18 barn, $^{nat/73}$Ge exhibits $\sigma_{inc} = 1.22$ barn. The Ge self-diffusion coefficients are equal within error limits, even for samples of identical chemical composition exhibiting different incoherent neutron scattering cross sections. The line represents a fit with an Arrhenius law. For comparison a Ge self-diffusion coefficient reported based upon crystal growth [44] (blue triangle), as well as a Ge self-diffusion coefficient (yellow triangle) and a Si self-diffusion coefficient (green triangle) reported based upon ab initio moleculardynmics simulations [45] for $Si_{50}Ge_{50}$ are shown.

diffusion in liquid Ge and $Ge_{80}Si_{20}$ is identical within the error limits. Moreover, the temperature dependence can be well described by an Arrhenius law over the entire temperature range: $D(T) = D_0 \exp(-E_A/k_BT)$ with $E_A = 164 \pm 8$ meV. The diffusion coefficients determined in this work are slightly higher than those reported in Ref. [32] at similar temperatures. Moreover, different from the results of Ref. [32], our data are well described by an Arrhenius law in the full temperature range down to the lowest temperatures. The reason for these differences is discussed in the footnote No. 5 of Ref. [22]. Hence we find no indications for a structurally induced change of the diffusion mechanism as suggested in Ref. [32]. For comparison a Ge self-diffusion coefficient inferred from the crystal growth behavior in $Si_{50}Ge_{50}$ is depicted in Fig. 2 as well [44]. The value lies approximately 40% below the Ge

TABLE I. Ge self-diffusion coefficients in liquid Ge [22,23] and $Si_{20}Ge_{80}$ measured using QNS on samples containing only ^{nat}Ge or a 1:1 $^{nat/73}$Ge isotope mixture.

sample	T (K)	$D(10^{-8}$ m^2/s)
$^{nat/73}$Ge	1223	1.34 ± 0.07
	1273	1.38 ± 0.07
	1350	1.58 ± 0.08
	1430	1.66 ± 0.09
	1520	1.77 ± 0.11
Si_{20} $^{nat/73}Ge_{80}$	1430	1.69 ± 0.12
	1520	1.84 ± 0.15
Si_{20} $^{nat}Ge_{80}$	1520	1.76 ± 0.15
	1573	1.84 ± 0.15
	1633	1.97 ± 0.12
	1693	1.84 ± 0.15

self-diffusion coefficients measured in this work for $Si_{20}Ge_{80}$. In Ref. [45], *ab initio* molecular-dynamics simulations of liquid $Si_{50}Ge_{50}$ are presented. Compared with the Ge self-diffusion coefficient we measured for liquid $Si_{20}Ge_{80}$ the reported Ge self-diffusion coefficient is slightly lower and the Si self-diffusion coefficient is slightly higher. However, compared with densely packed liquids of metallic elements or alloys that typically show diffusion coefficients in the order of magnitude of 10^{-10}–10^{-9} m^2/s at temperatures close to the melting temperature [5,25,26,39], the diffusion coefficients found for pure molten Ge and Si-Ge alloy melts are significantly higher. Moreover, the activation energy for self-diffusion is significantly smaller for liquids of Ge and Ge-Si as compared to those reported for melts of densely packed metals (e.g., 470 ± 30 meV for liquid Ni [26] or 640 ± 20 meV for $Zr_{64}Ni_{36}$ [46]). This faster atomic dynamics observed for the melts of Ge and Ge-Si is well in line with the considerably lower density of packing of the molten semiconductors.

IV. DIFFRACTION STUDIES ON LIQUID Ge AND $Ge_{80}Si_{20}$

Static structure factors $S(q)$ in liquid Ge and $Ge_{80}Si_{20}$ were measured using neutron diffraction on the high-intensity two-axis diffractometer D20 of the Institut Laue-Langevin (ILL) in Grenoble, France, using an incoming wavelength of 0.94 Å. A detailed description of data treatment and experimental setup is given in Ref. [41]. Moreover total x-ray structure factors of $Si_{20}Ge_{80}$ were measured using synchrotron radiation of 100 keV energy at the beamline BW5 of the Hasylab at DESY in Hamburg, Germany. The experimental setup is as described in Ref. [10]. Calibrated and dark current corrected one-dimensional intensity profiles as a function of the momentum transfer, q, have been calculated from the measured two-dimensional intensity data by using the FIT2D [47,48] software package. From these the total x-ray structure factors, are determined after subtraction of the background measured with the empty levitator, and correcting for self-absorption, Compton scattering, multiple scattering, polarization, and oblique incidence by utilizing the PDFGETX2 [49] analysis software.

Ge structure factors were measured by neutron diffraction at six different temperatures. For the first time a Ge structure factor was measured in the metastable regime of the undercooled melt $T = 1175$ K, approximately 40 K below the melting point. The highest temperature reached was $T = 1900$ K, several hundred degrees above the melting point of 1211 K. The structure factors are displayed in Fig. 3. A shoulder on the high q side of the first diffraction maximum at approximately 3 Å is clearly visible that is increasingly pronounced with decreasing temperature.

Fourier transformation of $S(q)$ yields the pair correlation functions $g(r)$ that are displayed in Fig. 4 for three different temperatures. The pair correlation functions show a weak dependence on the temperature with the main maxima becoming sharper with decreasing temperature. The positions of the first maxima in $g(r)$ correspond to the mean nearest-neighbor distance d_{NN}. Because later we will discuss the short-range order of binary Ge-Si melts, already here we use the typical nomenclature that refers to the partial pair correlation functions of alloy melts and the neighbor distances inferred from these (please consider pure Ge a Ge-Si alloy with vanishing Si content). In Table III the positions, q_1 and q_2 of the first and the second maximum in $S(q)$ and d_{NN} are listed.

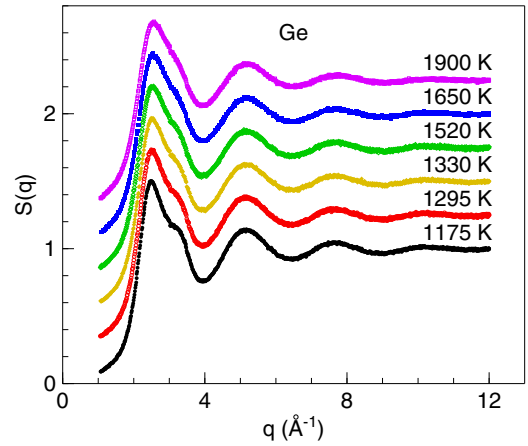

FIG. 3. Static structure factor $S(q)$ for liquid Ge over a broad temperature range from approximately 40 K below to 700 K above the melting point (1211 K). A shoulder on the high q-side of the first diffraction maximum (≈ 3.3 Å) is clearly visible, decreasingly strong with increasing temperature.

Our values agree well with reported values determined by neutron and x-ray diffraction [17,18,50–53]. However, the reported results of x-ray diffraction measurements at $T = 1253$ K [54] gave slightly larger d_{NN} values as compared with our neutron data. The position of the first maximum of the structure factor, q_1, slightly decreases with decreasing temperature. This tendency is also found in Ref. [52]. Nevertheless, due to the strong asymmetry of the first maxima of the structure factor, this shift of the maximum position in $S(q)$ does not necessarily indicate an increase of the mean nearest-neighbor distances with decreasing temperature. Indeed, the mean nearest-neighbor distance d_{NN} remains constant within the error limits (see Table III).

The first shell coordination number Z_{NN} is obtained by integrating the radial distribution function $n(r) = 4\pi\rho r^2 g(r)$ over the limits of the first peak. Using the macroscopic density of liquid Ge taken from Ref. [55], values closely around $Z_{NN} = 6.3 \pm 0.5$ are obtained that show no significant

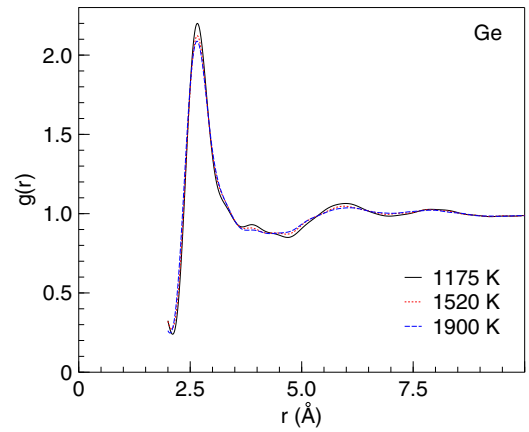

FIG. 4. Pair correlation functions $g(r)$ for liquid Ge.

TABLE II. Weightings of the partial structure factors in the different measured total $S(q)$. (A = Si, B = Ge) For the case of x-ray diffraction the values at $q = 2.5$ Å^{-1} are given, which corresponds roughly to the position of the first maximum of the structure factor.

	$\frac{\overline{b}^2}{\overline{b^2}}$	$\frac{c_A c_B(\overline{b_A}-\overline{b_B})^2}{\overline{b^2}}$	$\frac{2(\overline{b_A}-\overline{b_B})\overline{b}}{\overline{b^2}}$	$\frac{c_A^2\overline{b_A}^2}{\overline{b^2}}$	$\frac{c_B^2\overline{b_B}^2}{\overline{b^2}}$	$\frac{2c_A c_B\overline{b_A b_B}}{\overline{b^2}}$
Si_{20} $^{73}Ge_{80}$	0.995	0.005	0.365	0.029	0.683	0.282
Si_{20} $^{73/nat}Ge_{80}$	0.975	0.025	0.780	0.018	0.728	0.229
Si_{20} $^{nat}Ge_{80}$	0.954	0.046	1.044	0.012	0.752	0.191
Si_{20} Ge_{80} x-ray	0.926	0.074	1.313	0.007	0.772	0.146

dependence on the temperature. Compared to liquids of pure metals with typical coordination numbers of approximately twelve, this value is significantly lower (see Ref. [19] for liquid Ni, Fe, and Zr). Numerous classical [56,57] and *ab initio* MD simulations [33,34,58–60] of the static structure of liquid Ge are reported in literature. The simulated structure factors generally agree fairly well with the ones reported here. However, the structure factor calculated by Kulkarni *et al.* [34] at $T = 2000$ K shows a symmetric first maximum without a shoulder on the high q side. In contrast, our structure factor measured at the highest temperature ($T = 1900$ K) exhibits an asymmetric first diffraction maximum, although the shoulder is less pronounced at higher temperatures. Moreover, the short-range order was investigated for liquid $Si_{20}Ge_{80}$ at $T = 1650$ K, using isotopic substitution. The three different samples contained either ^{73}Ge, ^{nat}Ge or a 1:1 mixture of both, exhibiting a neutron scattering length of 5.02, 8.19, and 6.60 fm, respectively. Si exhibits a scattering length of 4.149 fm. In addition to the total structure factors measured with neutron scattering and isotopic substitution, the total x-ray structure factor has been determined by diffraction of synchrotron radiation, providing an even higher relative scattering power of the Ge component as for the neutron scattering experiments on the specimen containing Ge of natural isotopic abundance.

In Fig. 5(a), the measured total structure factors are depicted. A shoulder on the first diffraction maximum is clearly visible in all of the measured total structure factors. While the overall shape of all total structure factors is very similar to the one observed for liquid Ge, a systematic variation of the shape is observed such that with increasing relative scattering power of the Ge component the amplitudes of the oscillations increase and the intensity maxima are slightly shifted to smaller momentum transfer. This shift may be explained by the larger atomic size of the Ge atoms as compared with that of the Si atoms.

In Fig. 5(b), total structure factors measured by x-ray diffraction for liquid Si_{20} $^{nat}Ge_{80}$ at different temperatures in the range between 1380 and 1690 K (melting temperature $T_m = 1403$ K) are depicted. Again, only a weak temperature dependence is found. For a detailed investigation of the short-range order in a binary A-B melt, partial static structure factors may be calculated from three independent total static structure factors in the framework of the Bathia-Thornton [61] or the Faber-Ziman formalism [62]. In case of the Bhatia-Thornton formalism three partial static structure factors are defined: $S_{NN}(q)$ describes the topological short-range order of the liquid, $S_{CC}(q)$ its chemical short-range order, and $S_{NC}(q)$

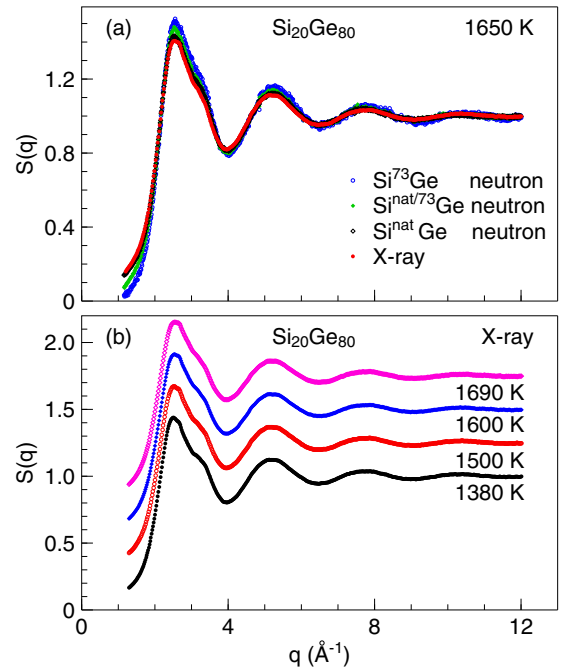

FIG. 5. (a) Total static structure factors measured using neutron diffraction on liquid Si_{20} $^{73}Ge_{80}$, Si_{20} $^{nat/73}Ge_{80}$, and Si_{20} $^{nat}Ge_{80}$ as well as by x-ray diffraction on a sample of natural isotopic abundance at $T = 1650$ K. A shoulder on the high q side of the first structure factor maximum is clearly visible and the overall shape of the total structure factors is very similar. (b) Total structure factor for liquid $Si_{20}Ge_{80}$ measured by x-ray diffraction at different temperatures. Successive curves have been offset by 0.2 for clarity.

the correlation of number density and chemical composition. In case of the Faber-Ziman formalism the three partial static structure factors $S_{AA}(q)$, $S_{BB}(q)$, and $S_{AB}(q)$ describe the contributions to $S(q)$ that result from the three different types of atomic pairs (A-A, B-B, and A-B). The relations are given by the following equations:

$$S(q)^{BT} = \frac{\overline{b}^2}{\overline{b^2}} S_{NN}(q) + \frac{c_A c_B(\overline{b_A}-\overline{b_B})^2}{\overline{b^2}} S_{CC}(q) + \frac{2(\overline{b_A}-\overline{b_B})\overline{b}}{\overline{b^2}} S_{NC}(q) \quad (3)$$

and

$$S(q)^{FZ} = \frac{c_A^2\overline{b_A}^2}{\overline{b^2}} S_{AA}(q) + \frac{c_B^2\overline{b_B}^2}{\overline{b^2}} S_{BB}(q) + \frac{2c_A c_B\overline{b_A b_B}}{\overline{b^2}} S_{AB}(q) + 1 - \frac{\overline{b}^2}{\overline{b^2}}. \quad (4)$$

Here c_A and c_B denote the concentration of the atoms of type A and B. b_A and b_B are the coherent scattering lengths of the atoms/isotopes, ($\overline{b} = c_A\overline{b_A} + c_B\overline{b_B}$ and $\overline{b^2} = c_A\overline{b_A^2} + c_B\overline{b_B^2}$). Similar equations hold for x-ray diffraction, if the neutron scattering lengths are replaced by the atomic scattering factors, $f(q)$. The weightings of the partial structure factors in the different measured total $S(q)$ are shown in Table II.

TABLE III. Structural properties of liquid Ge and $Si_{20}Ge_{80}$ measured using neutron- and x-ray diffraction, including positions of the first, q_1, and second, q_2, maxima in the topological structure factor $S_{NN}(q)$, the nearest-neighbor distances d_{NN}, d_{GeGe}, d_{GeSi}, and the partial coordination numbers Z_{NN}, Z_{GeGe}, Z_{GeSi}.

sample	T (K)	q_1 (Å^{-1})	q_2 (Å^{-1})	d_{NN} (Å)	Z_{NN}	d_{GeGe} (Å)	Z_{GeGe}	d_{GeSi} (Å)	Z_{GeSi}	Z_{SiGe}
Ge	1175	2.49 ± 0.01	5.17 ± 0.05	2.66 ± 0.02	6.4 ± 0.5	$= d_{NN}$	$= Z_{NN}$			
	1295	2.49 ± 0.01	5.15 ± 0.05	2.66 ± 0.02	6.3 ± 0.5	$= d_{NN}$	$= Z_{NN}$			
	1430	2.52 ± 0.01	5.12 ± 0.05	2.66 ± 0.02	6.4 ± 0.5	$= d_{NN}$	$= Z_{NN}$			
	1520	2.52 ± 0.01	5.17 ± 0.05	2.66 ± 0.02	6.2 ± 0.5	$= d_{NN}$	$= Z_{NN}$			
	1650	2.54 ± 0.01	5.17 ± 0.05	2.66 ± 0.02	6.4 ± 0.5	$= d_{NN}$	$= Z_{NN}$			
	1900	2.57 ± 0.01	5.20 ± 0.05	2.65 ± 0.02	6.4 ± 0.5	$= d_{NN}$	$= Z_{NN}$			
$Si_{20}Ge_{80}$	1650	2.55 ± 0.01	5.28 ± 0.05	2.60 ± 0.02	6.8 ± 0.5	2.69 ± 0.02	4.9 ± 0.5	2.55 ± 0.02	6.5 ± 0.5	1.6 ± 0.5
	1405					2.69 ± 0.02	4.9 ± 0.5	2.54 ± 0.02	6.3 ± 0.5	1.6 ± 0.5

It is noteworthy that the neutron scattering signal of the sample prepared with the ^{73}Ge isotope is dominated by the partial structure factor S_{NN} such that the total structure factor determined from this sample already gives a good approximation of S_{NN}. The prefactors of the partial structure factors S_{CC} and S_{SiSi} are very small for all experiments, such that the influence of S_{CC} or S_{SiSi} on the measured total structure factors is comparable or even smaller than the experimental error. The determination of these partial structure factors from the measured total structure factors is not possible and the attempt to solve the equation system (3) or (4) using the data from three independent measurements as an input in order to determine all three partial structure factors gives strongly oscillating results for S_{SiSi} and S_{CC} that are obviously incorrect. The unrealistic strong oscillations of these partial structure factors compromise also the precision of the other partial structure factors calculated by means of this.

Nevertheless, it is possible to determine good approximations of the other partial structure factors. Taking into consideration the very small prefactors of S_{CC} for neutron scattering experiments on the samples prepared with ^{73}Ge and with the isotopic mixture of ^{73}Ge and ^{nat}Ge, it is reasonable to neglect the contribution of S_{CC} to these total structure factors. Hence we assume that S_{CC} has a constant value of 1 in order to assure the right asymptotic behavior of the structure factors at large momentum transfer. This allows for calculation of good approximations of S_{NN} and S_{NC} from the two sets of experimental data (Si_{20} $^{73}Ge_{80}$ and Si_{20} $^{nat/73}Ge_{80}$) by solving of the equation system (3). Within the Faber-Ziman formalism the coefficients of S_{SiSi} are very small for the x-ray diffraction experiment and the neutron scattering experiment on the sample prepared with Ge of natural isotopic composition. Again neglecting this contributions allows to calculate good approximations of S_{GeGe} and S_{GeSi} from the two total structure factors by solving the equation system (4). The partial structure factors S_{NN}, S_{NC}, S_{GeGe}, and S_{GeSi} that have been determined at a temperature of 1650 K by means of the approximations described before are depicted in Fig. 6(a). The partial structure factor S_{NN} is nearly identical to the total structure factor measured for the sample containing ^{73}Ge, which is expected in the light of the coefficients given in Table II. Its shape strongly resembles the shape of the structure factor of pure Ge at same temperature (Fig. 3). Interestingly, the partial Faber-Ziman structure factor S_{GeGe} does not show the characteristic shoulder that appears on the high-q side of the first intensity maximum of S_{NN} and also for the structure factor of pure Ge. S_{GeSi}, however shows a maximum at the position of this shoulder. From this it can be concluded that when alloying Ge with Si, the Si atoms are taking preferentially such atomic positions that together with their Ge neighbors give rise to the shoulder in the structure factors. The shoulder appearing on the high-q side of the first intensity maximum corresponds to shorter than average nearest-neighbor distances in real space. This can be directly seen in the corresponding partial pair correlation functions $g_{NN}(r)$, $g_{GeGe}(r)$, and $g_{GeSi}(r)$ at $T = 1650$ K that are depicted in Fig. 6(b) together with the pair correlation function of pure Ge. While the high-r tails of first maxima of g_{GeGe} and of the pair correlation function of pure Ge are identical, at smaller distances the maximum of g_{GeGe}

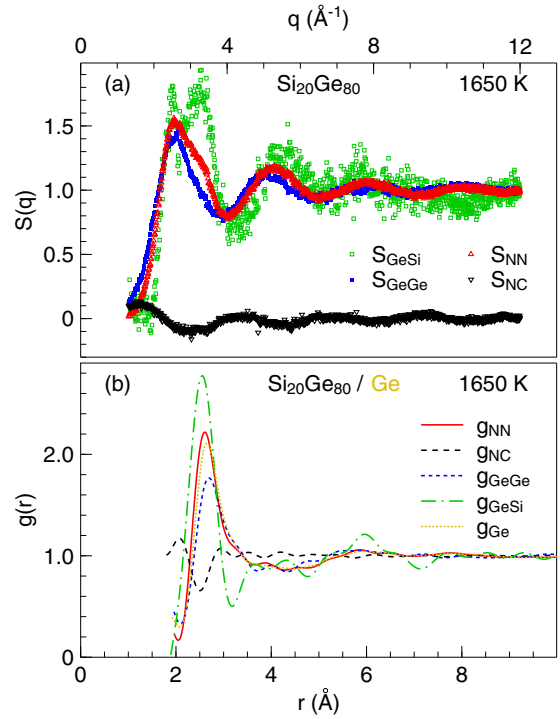

FIG. 6. (a) Partial structure factors $S_{NN}(q)$, $S_{NC}(q)$, $S_{GeGe}(q)$, and $S_{GeSi}(q)$ for liquid $Si_{20}Ge_{80}$ at a temperature of $T = 1650$ K. (b) Corresponding partial pair correlation functions $g_{NN}(r)$, $g_{NC}(r)$, $g_{GeGe}(r)$, and $g_{GeSi}(r)$. Also shown is the pair correlation function of liquid Ge.

is considerably smaller as compared with the melt of pure Ge. Instead, here the maximum of g_{GeSi} is located. This preference of the Si atoms to substitute during alloying those Ge-atoms with a small neighbor distance may be understood in the light of the smaller atomic size of the Si atoms. From the partial Faber-Ziman pair correlation functions partial coordination numbers of $Z_{GeGe} = 4.8$, $Z_{GeSi} = 6.4$, and $Z_{SiGe} = 1.6$ are obtained.

In Table III, the (partial) nearest-neighbor distances, d_{NN}, d_{GeGe}, and d_{GeSi} as well as the corresponding (partial) coordination numbers Z_{NN}, Z_{GeGe}, Z_{GeSi}, and Z_{SiGe} are compiled for liquid Ge-Si and Ge at different temperatures. Compared with pure Ge, for the $Ge_{80}Si_{20}$ alloy the peak positions in $S_{NN}(q)$ and $g_{NN}(r)$ are shifted slightly towards higher q and respectively lower r values for the latter. Using the measured number density data taken from Ref. [55] for the close composition $Ge_{75}Si_{25}$ (the composition dependence of the number density in Ge-Si is rather low) a nearest-neighbor coordination number of $Z_{NN} = 6.8 \pm 0.5$ is derived.

Within the error limits the coordination number of liquid $Si_{20}Ge_{80}$ agrees with the one of liquid Ge. Accordingly its value is significantly lower than that of typical liquid metals. Apparently the topological arrangements in liquid Ge and $Si_{20}Ge_{80}$ are very similar, with slightly shorter interatomic distances for the latter. To the best of the authors knowledge, only total structure factors for liquid Si-Ge were reported in literature. In Ref. [20], energy dispersive x-ray diffraction measurements on liquid Ge, $Si_{30}Ge_{70}$, $Si_{50}Ge_{50}$, and Si are reported and in Ref. [17] x-ray diffraction investigations on liquid Ge, $Si_{25}Ge_{75}$, $Si_{50}Ge_{50}$, $Si_{75}Ge_{25}$, and Si are presented. Neutron diffraction measurements on liquid $Si_{50}Ge_{50}$ are reported in Ref. [21] for which samples prepared with elements of natural isotopic abundance have been used. As discussed before, in both cases, the Ge-Ge correlations provide the strongest contribution to the scattered signal. Also in these cases a shoulder is clearly visible on the high-q side of the first structure factor maximum.

For liquid Ge, average nearest-neighbor distances of roughly 2.74–2.76 Å are reported in Ref. [20] and of 2.68–2.69 Å in Ref. [17]. Despite the fact that it is questionable to calculate interatomic distances from total pair correlation functions, the nearest-neighbor distances reported for $Si_{25}Ge_{75}$, $Si_{30}Ge_{70}$, $Si_{50}Ge_{50}$, and $Si_{75}Ge_{25}$ are slightly smaller as compared with pure Ge [17,20]. For liquid Si, considerably lower values of 2.45–2.49 Å are reported [17,20]. The reported value of 2.66 Å for $Si_{25}Ge_{75}$ is close to the d_{GeGe} = 2.69 Å we found for liquid $Ge_{80}Si_{20}$, which is expected due to the significantly higher scattering cross section of Ge as compared with that of Si in x-ray diffraction experiments. The decrease of the interatomic distances when adding Si to Ge that is inferred from total pair correlation functions is well in line with the smaller d_{NN} we find for $Ge_{80}Si_{20}$ as compared with that of pure Ge (see Table III). It is mainly due to the shorter Ge-Si distances d_{GeSi}, while d_{GeGe} is even slightly larger as for pure Ge. The latter effect is mainly due to the selective substitution of positions with a smaller interatomic distance by the smaller Si atoms. When deceasing the temperature to 1405 K, g_{GeGe} remains essentially unchanged (Fig. 7). Consequently also d_{GeGe} and Z_{GeGe} are constant within the error limits. g_{GeSi}, however, becomes significantly

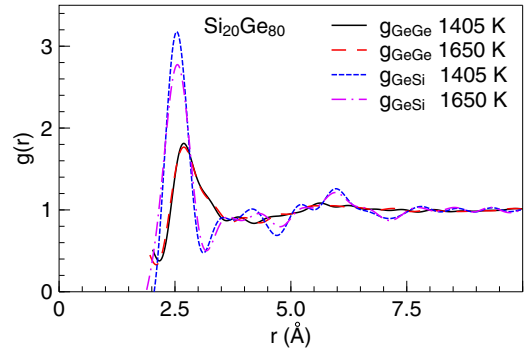

FIG. 7. Partial pair correlation functions $g_{GeGe}(r)$ and $g_{GeSi}(r)$ at temperatures of $T = 1650$ and 1405 K.

sharper towards lower temperatures. Because the increase of the height of the peak is associated with a decrease of the width, the partial coordination number Z_{GeSi} is not changed. This may indicate that within the investigated temperature range the changes of the structure factors as a function of the temperature are mainly due to Debye-Waller like influences on the partial structure factors rather than by a fundamental change of the short-range order as suggested by Refs. [32,34]. The temperature dependence of the sharpness of the intensity maxima is considerably stronger for the Ge-Si neighbor pairs as compared with the Ge-Ge pairs. Taking into consideration that the Si atoms take atomic positions that are responsible for the appearance of the characteristic shoulder on the first maximum of the structure factor, this mechanism also explains why this shoulder fades out at high temperatures, while the asymmetry of the maximum remains. This conclusion was inferred from the analysis of the partial structure factors in the $Ge_{80}Si_{20}$. Nevertheless it should also provide an explanation of the same observation in pure liquid Ge. In the cluster-based structural model for liquid Ge suggested by Ashcroft [30], the maximum of the structure factor is associated with intercluster correlations between tetrahedral clusters while the shoulder is suggested to result from intracluster correlations. Our findings, however, suggest that the short-range structure of the melt is characterized by at least (unfortunately we were not able to determine g_{SiSi}) two different distinct nearest-neighbor distances that give rise to a peak splitting of $S(q)$ and hence to the characteristic shoulder. This conclusion becomes apparent in the light of the distinct chemical short-range order as described by partial structure factors that is introduced when substituting Ge by Si, while the topological short-range order is not affected by the substitution.

The existence of two different distinct nearest-neighbor distances may be compatible with a hypothesis raised in Ref. [17] that in Ge-Si liquids occurs some kind of continuous phase transition from a high density and a low density liquid when decreasing the temperature. Nevertheless, we find that the partial coordination numbers remain constant as a function of the temperature, while the observed changes of the shape of the structure factors result from a more pronounced Debye-Waller like broadening of S_{GeSi} with increasing temperature as compared with that of S_{GeGe}. Hence, we observe no fundamental changes of the short-range structure that should occur

in case of the suggested liquid-liquid phase transformation from a high density to a low density liquid.

For liquid $Si_{50}Ge_{50}$, *ab intio* MD simulations show a slight preference for phase separation [45]. From the temperature dependence of the partial pair correlation functions g_{GeGe} and g_{GeSi} and the partial coordination numbers Z_{GeGe} and Z_{GeSi} we find no indications for such a demixing tendency in $Ge_{80}Si_{20}$.

The very similar topological structure with almost identical coordination numbers in pure Ge and $Si_{20}Ge_{80}$ provides a structural explanation for our finding that the measured self-diffusion coefficients in liquid Ge and $Si_{20}Ge_{80}$ are identical within error limits at same temperature.

V. CONCLUSION

We studied structure and dynamics in liquid Ge and $Si_{20}Ge_{80}$ using neutron scattering and x-ray diffraction. QNS was employed to obtain Ge self-diffusion coefficients in liquid $Si_{20}Ge_{80}$ over a temperature range of 30 K to 300 K above the liquids temperature. The Ge self-diffusion coefficients are equal within the errors limits to the Ge self-diffusion coefficients in liquid Ge [22,23]. The temperature dependence is well described by an Arrhenius law with an activation energy of 164 ± 8 meV within the entire temperature range. As compared with the atomic dynamics of densely packed metallic melts, liquid Ge and Ge-Si show a considerably higher atomic mobility.

In addition, static structure factors were measured using neutron and x-ray diffraction in combination with containerless processing employing EML. Structure factors of liquid Ge were measured over a broad temperature range from 40 K below to several hundred K above the melting point. A shoulder on the high-q side of the first structure factor maximum is observed that becomes less pronounced with increasing temperature. Furthermore, by using the isotopic substitution method and by combination with x-ray diffraction good approximations of the partial structure factors S_{NN}, S_{NC}, S_{GeGe}, and S_{GeSi} of liquid $Si_{20}Ge_{80}$ were determined. The topological structure factors S_{NN} for $Si_{20}Ge_{80}$ resemble the structure factors of pure Ge, indicating a similar topological short-range order.

A coordination number of about 6.3 ± 0.5 in the case of liquid Ge and 6.8 ± 0.5 for liquid $Si_{20}Ge_{80}$ was derived. Both are significantly lower than for densely packed metallic liquids. The resulting low packing density of these melts provides an explanation for the considerably faster atomic dynamics observed for liquid Ge and Ge-Si as compared to those of densely packed metallic melts. Moreover, the similarities in the topological short-range order of liquid $Ge_{80}Si_{20}$ and pure Ge explain the similar Ge self-diffusion behavior in both systems.

ACKNOWLEDGMENTS

We would like to thank I. Kaban, T. Kordel, N. Mattern, and O. Shuleshova for fruitful discussion and help during the experiments.

[1] Y. Q. Cheng, H. W. Sheng, and E. Ma, Phys. Rev. B **78**, 014207 (2008).
[2] N. Jakse and A. Pasturel, Appl. Phys. Lett. **105**, 131905 (2014).
[3] S. Hao, C. Z. Wang, M. J. Kramer, and K. M. Ho, J. Appl. Phys. **107**, 053511 (2010).
[4] A. E. Lagogianni, J. Krausser, Z. Evenson, K. Samwer, and A. Zaccone, J. Stat. Mech.: Theor. Exp. (2016) 084001.
[5] D. Holland-Moritz, B. Nowak, F. Yang, and A. Meyer, Pure Appl. Chem. **91**, 895 (2019).
[6] W. Götze, *Complex Dynamics of Glass-Forming Liquids: A Mode-Coupling Theory* (Oxford University Press, Oxford, 2008).
[7] B. Nowak, D. Holland-Moritz, F. Yang, T. Voigtmann, T. Kordel, T.C. Hansen, and A. Meyer, Phys. Rev. Materials **1**, 025603 (2017).
[8] B. Nowak, D. Holland-Moritz, F. Yang, T. Voigtmann, Z. Evenson, T.C. Hansen, and A. Meyer, Phys. Rev. B **96**, 054201 (2017).
[9] D. Holland-Moritz, S. Stüber, H. Hartmann, T. Unruh, T. Hansen, and A. Meyer, Phys. Rev. B **79**, 064204 (2009).
[10] D. Holland-Moritz, F. Yang, T. Kordel, S. Klein, F. Kargl, J. Gegner, T. Hansen, J. Bednarcik, I. Kaban, O. Shuleshova, N. Mattern, and A. Meyer, Europhys. Lett. **100**, 56002 (2012).
[11] F. Yang, D. Holland-Moritz, J. Gegner, P. Heintzmann, F. Kargl, C. C. Yuan, G. G. Simeoni, and A. Meyer, Europhys. Lett. **107**, 46001 (2014).
[12] S. Stüber, D. Holland-Moritz, T. Unruh, and A.Meyer, Phys. Rev. B **81**, 024204 (2010).
[13] S. Nell, F. Yang, Z. Evenson, and A. Meyer, Phys. Rev. B **103**, 064206 (2021).
[14] A. Meyer, L. Hennig, F. Kargl, and T. Unruh, J. Phys.: Condens. Matter **31**, 395401 (2019).
[15] H. S. Schnyders and J. B. V. Zytveld, J. Phys.: Condens. Matter **8**, 10875 (1996).
[16] N. E. Cusack, Rep. Prog. Phys. **26**, 361 (1963).
[17] I. Pozdnyakova, O. Roik, J. W. E. Drewitt, A. Bytchkov, F. Kargl, S. Jahn, S. Brassamin, and L. Hennet, J. Phys.: Condens. Matter **33**, 244002 (2021).
[18] P. S. Salmon, J. Phys. F: Met. Phys **18**, 2345 (1988).
[19] T. Schenk, D. Holland-Moritz, V. Simonet, R. Bellissent, and D. M. Herlach, Phys. Rev. Lett. **89**, 075507 (2002).
[20] Y. Naito, M. Inui, T. Anai, and K. Tamura, J. Non-Cryst. Solids **353**, 3376 (2007).
[21] S. Krishnan, L. Hennet, T. Key, B. Glorieux, M.-L. Saboungi, and D. L. Price, J. Non-Cryst. Solids **353**, 2975 (2007).
[22] H. Weis, F. Kargl, M. Kolbe, M. M. Koza, T. Unruh, and A. Meyer, J. Phys.: Condens. Matter **31**, 455101 (2019).
[23] H. Weis, T. Unruh, and A. Meyer, High Temperatures-High Pressures **42**, 39 (2013).
[24] A. I. Pommrich, A. Meyer, D. Holland-Moritz, and T. Unruh, Appl. Phys. Lett. **92**, 241922 (2008).
[25] A. Meyer, Phys. Rev. B **81**, 012102 (2010).

[26] A. Meyer, S. Stüber, D. Holland-Moritz, O. Heinen, and T. Unruh, Phys. Rev. B **77**, 092201 (2008).
[27] D. Holland-Moritz, S. Stüber, H. Hartmann, T. Unruh, and A. Meyer, J. Phys.: Conf. Ser. **144**, 012119 (2009).
[28] A. Meyer, Phys. Rev. B **66**, 134205 (2002).
[29] A. Meyer, W. Petry, M. Koza, and M.-P. Macht, Appl. Phys. Lett. **83**, 3894 (2003).
[30] N. W. Ashcroft, Il Nuovo Cimento D **12**, 597 (1990).
[31] S. Hosokawa, Y. Kawakita, W.-C. Pilgrim, and H. Sinn, Phys. Rev. B **63**, 134205 (2001).
[32] S. M. Chathoth, B. Damaschke, T. Unruh, and K. Samwer, Appl. Phys. Lett. **94**, 221906 (2009).
[33] G. Kresse and J. Hafner, Phys. Rev. B **49**, 14251 (1994).
[34] R. V. Kulkarni, W. G. Aulbur, and D. Stroud, Phys. Rev. B **55**, 6896 (1997).
[35] J. Horbach, S. K. Das, A. Griesche, M.-P. Macht, G. Frohberg, and A. Meyer, Phys. Rev. B **75**, 174304 (2007).
[36] A. Griesche, M.-P. Macht, S. Suzuki, K.-H. Kraatz, and G. Frohberg, Scripta Mater. **57**, 477 (2007).
[37] C. Barat and J. P. Garandet, Int. J. Heat Mass Transfer **39**, 2177 (1996).
[38] F. Kargl, E. Sondermann, H. Weis, and A. Meyer, High Temperatures-High Pressures **42**, 3 (2013).
[39] F. Kargl, H. Weis, T. Unruh, and A. Meyer, J. Phys.: Conf. Ser. **340**, 012077 (2012).
[40] H. E. Fischer, A. C. Barnes, and P. S. Salmon, Rep. Prog. Phys. **69**, 233 (2006).
[41] D. Holland-Moritz, T. Schenk, P. Convert, T. Hansen, and D. M. Herlach, Meas. Sci. Technol. **16**, 372 (2005).
[42] H. Kimura, M. Watanabe, K. Izumi, T. Hibiya, and D. Holland-Moritz, Appl. Phys. Lett. **78**, 604 (2001).
[43] J. P. Hansen and I. R. McDonald, *Theory of Simple Liquids* (Academic Press Inc., London, 1986).
[44] S. Adachia, Y. Ogata, N. Koshikawa, S. Matsumoto, K. Kinoshita, I. Yoshizaki, T. Tsuru, H. Miyata, M. Takayanagi, and S. Yoda, J. of Cryst. Growth **280**, 372 (2005).
[45] E. Ko, M. Jain, and J. R. Chelikowsky, J. Chem. Phys. **117**, 3476 (2002).
[46] T. Kordel, D. Holland-Moritz, F. Yang, J. Peters, T. Unruh, T. Hansen, and A. Meyer, Phys. Rev. B **83**, 104205 (2011).
[47] A. P. Hammersley, *FIT2D V9.129 Reference Manual V3.1, ESRF98HA01T* (ESRF Internal Report, Grenoble, 1998).
[48] A. P. Hammersley, S. Swensson, M. Hanfland, A. Fitch, and D. Hausermann, High Press. Res. **14**, 235 (1996).
[49] X. Qiu, J. Thompson, and S. Billinge, J. Appl. Crystallogr. **37**, 678 (2004).
[50] M. C. Bellissent-Funel, P. Chieux, D. Levesque, and J. J. Weis, Phys. Rev. A **39**, 6310 (1989).
[51] M. Davidovic, M. Stojic, and D. Jovic, J. Phys. C: Solid State Phys. **16**, 2053 (1983).
[52] J. P. Gabathuler and S. Steeb, Z. Naturforsch. **34a**, 1314 (1979).
[53] S. P. Isherwood and B. R. Orton, Phil. Mag. **17**, 561 (1968).
[54] Y. Waseda and K. Suzuki, Z. Physik B **20**, 339 (1975).
[55] S. M. Chathoth, B. Damaschke, K. Samwer, and S. Schneider, Appl. Phys. Lett. **93**, 071902 (2008).
[56] W. Yu, Z. Q. Wang, and D. Stroud, Phys. Rev. B **54**, 13946 (1996).
[57] A. Arnold, N. Mauser, and J. Hafner, J. Phys.: Condens. Matter **1**, 965 (1989).
[58] V. Hugouvieux, E. Farhi, M. R. Johnson, F. Juranyi, P. Bourges, and W. Kob, Phys. Rev. B **75**, 104208 (2007).
[59] N. Takeuchi and I. L. Garzon, Phys. Rev. B **50**, 8342 (1994).
[60] V. Godlevsky, J. R. Chelikowsky, and N. Troullier, Phys. Rev. B **52**, 13281 (1995).
[61] A. B. Bhatia and D. E. Thornton, Phys. Rev. B **2**, 3004 (1970).
[62] T. E. Faber and J. M. Ziman, Philos. Mag. **11**, 153 (1965).